

Tạp chí

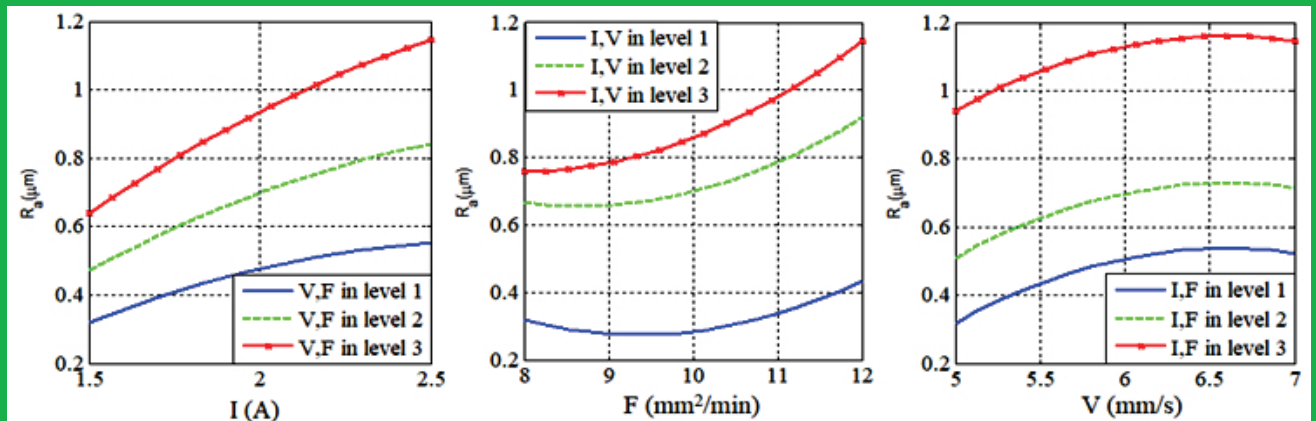
KHOA HỌC VÀ

CÔNG NGHỆ ỨNG DỤNG

JOURNAL OF APPLIED SCIENCE AND TECHNOLOGY

Số 48

Tháng 12/2025



MỤC LỤC

STT		Trang
1.	Nguyen Hong Phong, Van- The Tran, Thuan – Hoang Minh, and Vu Duc Phuc STATISTICAL MODELING AND OPTIMIZATION OF SURFACE ROUGHNESS IN WIRE EDM OF NONCIRCULAR GEARS MADE OF SKD11 STEEL Mô hình hóa thống kê và tối ưu hóa độ nhám bề mặt trong gia công EDM các bánh răng không tròn làm từ thép SKD11	5
2.	Trong-Tung Dam, Thi-Quy Vu, Xuan-Truong Vu, Dinh-Quan Doan VELOCITY-DEPENDENT DEFORMATION MECHANISM OF FENICRCOTI HIGH-ENTROPY ALLOY UNDER VIBRATION-ASSISTED MACHINING Cơ chế biến dạng phụ thuộc vận tốc của hợp kim entropy cao FeNiCrCoTi trong quá trình gia công hỗ trợ rung động	12
3.	Van-Duong Vuong, Minh-Thuan Hoang CUTTER CORRECTION METHOD FOR IMPROVING THE ACCURACY OF MANUFACTURED SCREW ROTOR BY END MILLING CUTTER Phương pháp hiệu chỉnh dụng cụ cắt để nâng cao độ chính xác gia công rotor trục vít bằng dao phay ngón	19
4.	Trong-Linh Nguyen, Anh-Vu Pham, Van-Thoai Nguyen ATOMISTIC INSIGHTS INTO Al/Al EXPLOSIVE WELDING: A MOLECULAR DYNAMICS STUDY OF INTERFACIAL BONDING AND DIFFUSION MECHANISMS Nghiên cứu ở cấp nguyên tử quá trình hàn nổ Al/Al bằng mô phỏng động lực học phân tử về cơ chế liên kết và khuếch tán tại giao diện	25
5.	Anh-Vu Pham, Trong-Linh Nguyen INDENTATION SIZE EFFECT ON THE DEFORMATION BEHAVIOR OF Ta-Cu AMORPHOUS THIN FILMS Ảnh hưởng của kích thước dụng cụ đến hành vi biến dạng của màng mỏng vô định hình Ta-Cu	32
6.	Nguyễn Thị Vân Anh, Nguyễn Hữu Cường, Đào Văn Đã, Đỗ Thành Hiếu NGHIÊN CỨU MÔ PHỎNG HỆ THỐNG QUANG ĐIỆN BA PHA NỐI LƯỚI SỬ DỤNG KỸ THUẬT ĐIỀU CHẾ SVPWM CHO NGHỊCH LƯU Simulation Study of A Three-Phase Grid-Connected Photovoltaic System using SVPWM Technique for The Inverter	38
7.	Giànn Thị Thu Hường, Cao Thị Hoài Thủy ĐÁNH GIÁ MỘT SỐ TÍNH CHẤT CƠ LÝ CỦA VẢI DỆT KIM ĐAN DỌC SỬ DỤNG SỢI POLYESTER TÁI CHẾ Evaluation of Some Mechanical Properties of Warp-Knitted Fabrics using Recycled Polyester Yarn	45
8.	Hà Ngọc Tuấn, Phạm Thị Ánh Hương, Trần Thị Thu Huyền, Ngô Thị Lan Anh SMOTE-ENSEMBLE: TỔNG QUAN KỸ THUẬT CÂN BẰNG DỮ LIỆU VÀ MÔ HÌNH HỌC MÁY KẾT HỢP TRONG DỰ ĐOÁN SỚM BIẾN CHỨNG VÔNG MẠC ĐÁI THÁO ĐƯỜNG Smote-Ensemble: A Review of Data-Balancing Techniques and Hybrid Machine Learning Models for Early Prediction of Diabetic Retinopathy Complications	51

9. **Nguyễn Đỗ Khải Hoàn, Trần Đỗ Thu Hà, Lưu Hoàng Minh, Nguyễn Xuân Mong, Nguyễn Văn Đạt, Trương Quốc Huy, Nguyễn Thanh Bình** 58
MỘT PHƯƠNG PHÁP TIẾP CẬN HIỆU QUẢ CHO BÀI TOÁN PHÁT HIỆN VẬT THỂ BAY TRÊN KHÔNG TẦM THẤP
An Effective Approach for Low-Altitude Aerial Object Detection
10. **Bui-Van HAI, Le-Duc HIEU, Nguyen-Phi TRUONG, Lam-Quang VINH, Khong-Van Nguyen** 62
THE IMPACT OF CERTAIN WORKING PARAMETERS ON THE DRILLING PROCESS OF PERCUSSIVE-ROTARY DRILLING
Ảnh hưởng của một số thông số làm việc đến quá trình khoan xoay đập
11. **Pham Thi Trang, Do Phuc Huong** 68
USING ROLE-PLAYING ACTIVITIES TO ENHANCE SPEAKING SKILLS OF SECOND-YEAR NON-ENGLISH MAJOR STUDENTS: AN ACTION RESEARCH AT A UNIVERSITY IN HUNG YEN
Sử dụng hoạt động nhập vai nhằm nâng cao kỹ năng nói cho sinh viên không chuyên ngữ năm thứ hai: nghiên cứu hành động tại một trường đại học ở Hưng Yên
12. **Nguyễn Anh Hải** 75
NGHIÊN CỨU VÀ CHẾ TẠO MẪU ROBOT TỰ HÀNH HỖ TRỢ CÔNG TÁC ĐÀO TẠO VỚI CHỨC NĂNG NHẬN DIỆN VÀ ĐỐI THOẠI THÔNG MINH
Research and Development of an Autonomous Mobile Robot for Educational Support with Intelligent Recognition and Dialogue Functions



ATOMISTIC INSIGHTS INTO Al/Al EXPLOSIVE WELDING: A MOLECULAR DYNAMICS STUDY OF INTERFACIAL BONDING AND DIFFUSION MECHANISMS

Trong-Linh Nguyen*, Anh-Vu Pham, Van-Thoai Nguyen*

Hung Yen University of Technology and Education

* Corresponding authors: tronglinh.skh@gmail.com, thoaidinh8586@gmail.com

Received: 16/10/2025

Revised: 10/11/2025

Accepted for publication: 12/12/2025

Abstract:

Explosive welding (EXW) is widely used to join similar and dissimilar metals, yet its atomistic mechanisms remain unclear. In this study, molecular dynamics simulations were performed to investigate aluminum–aluminum EXW using an embedded atom method potential. Results show that flyer impact causes temperature to exceed 2500 K and pressure to peak at ~27 GPa, inducing severe plastic deformation without bulk melting. Mean square displacement and concentration analyses reveal diffusion during loading, while unloading enables interfacial mixing, resulting in a thin diffusion layer of ~12 Å. Radial distribution function results confirm solid-state bonding dominated by plastic deformation and localized atomic rearrangement. These findings provide atomistic insights into Al–Al explosive welding, supporting process optimization for reliable similar-metal joints.

Keywords: *Explosive welding, Molecular dynamics simulation, Al–Al bonding, Interfacial diffusion.*

1. Introduction

Explosive welding (EXW) is a solid-state bonding technique in which two metals are joined by a high-velocity impact, typically initiated by the detonation of an explosive charge [1,2]. This process is advantageous for joining similar or dissimilar metals that are difficult to weld using traditional fusion-based methods [3]. Unlike fusion welding, EXW occurs in the solid state, thereby avoiding extensive heat-affected zones and minimizing the formation of brittle intermetallic compounds. While much of the existing research has focused on EXW of dissimilar metals such as Al–Cu or Ti–Al [4,5], there is increasing interest in understanding how similar metals such as aluminum–aluminum behave during high-speed impact welding at the atomic scale.

Molecular dynamics (MD) simulation is a powerful tool for exploring the underlying mechanisms of welding at nanometer and picosecond scales, including shock wave propagation, local plastic deformation, interface mixing, and atomic diffusion [6]. In this study,

MD simulations are performed to investigate explosive welding between two pure aluminum blocks. The process is modeled in six stages: energy minimization, thermal equilibration, high-velocity loading, unloading, controlled cooling, and final relaxation. The simulation uses an EAM potential specifically parameterized for aluminum, which reliably reproduces its structural and mechanical properties such as lattice constants, cohesive energy, and elastic constants. The goal of this work is to gain insight into the bonding process, stress evolution, and interfacial behavior during aluminum–aluminum explosive welding.

In addition to fundamental understanding, the present atomistic study provides practical implications for aluminum explosive welding. In particular, the relationships between impact velocity, interfacial plastic deformation, and localized atomic diffusion revealed in this work can be used as physical guidance for selecting suitable collision conditions in industrial Al/Al cladding processes. The identified roles of high-pressure suppression of melting and unloading-induced interfacial mixing

also provide insight for controlling joint quality and reducing interfacial defects in similar-metal explosive welding.

2. Methodology

The simulation model consists of two pure aluminum blocks aligned along the z-axis, with the flyer block positioned at the top and the stationary base block at the bottom. Each block is constructed using a face-centered cubic (FCC) lattice with a lattice constant of 4.05 Å, representative of aluminum at ambient conditions. The overall dimensions of the simulation box are 32.60 Å × 32.61 Å × 113.4 Å along the x, y, and z directions, respectively, comprising a total of 7168 atoms. The two blocks are initially separated by a 20 Å vacuum gap to facilitate high-velocity impact during the welding process.

Figure 1a illustrates the atomic structure colored by particle type, while Figure 1b shows the configuration colored by local crystal structure using the common neighbor analysis (CNA) method, confirming the perfect FCC arrangement in both blocks before impact. Fixed boundary layers are applied at the top and bottom to suppress translational motion and to implement reflective boundary conditions along the z-direction. Periodic boundary conditions are applied in the x and y directions. Interatomic interactions are described using the embedded atom method (EAM) potential for aluminum [7], which reliably reproduces the structural and mechanical properties of Al and has been widely used in molecular dynamics studies of deformation, dislocation behavior and welding processes.

After the initial construction, the whole system was first relaxed by energy minimization using the conjugate-gradient method to eliminate atomic overlaps and local stress concentrations. Subsequently, thermal equilibration was performed under the NPT ensemble at 300 K and 0 bar for 10 ps. A constant time step of 1.0 fs was used in all dynamic simulations. The equilibrated atomic configurations obtained after this NPT equilibration step were used as the initial configurations for the impact simulations and are shown in Figure 1.

The impact simulation was then carried out by assigning the flyer block an initial velocity of approximately $v_x \approx 3.47$ Å/ps and $v_z \approx -29.7$ Å/ps. The selected impact velocity is of the same order

as that commonly adopted in molecular dynamics simulations of explosive welding to reproduce shock pressures on the order of several tens of GPa and severe interfacial plastic deformation, as reported in previous studies [1]. The loading stage was performed under the NVE ensemble in order to preserve the natural shock response during high-velocity impact. During loading, the flyer bulk moves toward the base bulk, and when its thickness is reduced to the minimum length, the transition region of the flyer becomes fixed [1]. The loading duration was determined by the actual impact process and therefore varies depending on the collision evolution.

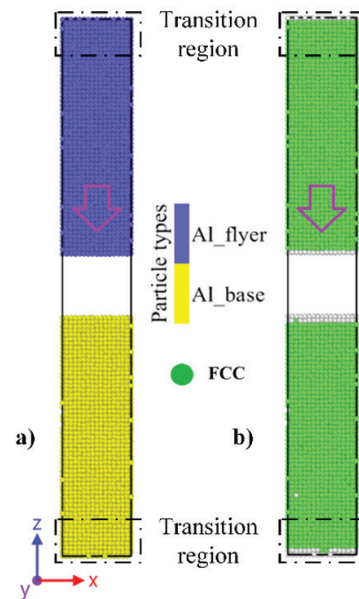


Figure 1. Initial atomic configurations for the Al–Al explosive welding simulation after energy minimization and NPT equilibration at 300 K and 0 bar: (a) atomic structure colored by particle type and (b) atomic configuration colored by crystal structure using CNA.

After loading, the system undergoes controlled unloading under the NPT ensemble, gradually reducing the temperature from its peak value back to 300 K. This is followed by a final relaxation stage at 300 K and 0 bar for 100 ps to allow the system to reach equilibrium. During all NPT stages, temperature and pressure were regulated using a Nosé–Hoover thermostat and barostat. The thermostat and barostat damping parameters were set to $T_{damp}=1.0$ ps and $P_{damp}=0.05$ ps during

the equilibration stage, and to $T_{damp}=1.0$ ps and $P_{damp}=1.0$ ps during the cooling and relaxation stages. The complete simulation stages and key parameters are summarized in Table 1.

The equations of motion were integrated using the velocity-Verlet algorithm implemented in LAMMPS. Throughout the simulation, LAMMPS computes are used to extract atomic stresses (stress/atom), Mean Square Displacements (MSD), and partial temperatures (temp/partial). Structural data and atomic configurations are saved periodically for visualization and post-analysis using OVITO.

3. Results and discussion

Figure 2 shows the evolution of temperature and pressure in the simulation system during the loading stage of the explosive welding process. At the onset of flyer impact (around 0 ps), both temperature and pressure exhibit a sharp increase due to the intense kinetic energy conversion into internal energy. The temperature rapidly rises to above 2500 K, while the pressure peaks at approximately 27 GPa.

Following this initial spike, both temperature and pressure undergo fluctuations during the early unloading phase (0–20 ps), which are associated with shock wave propagation, atomic rearrangement, and partial relaxation of the system. These oscillations gradually decay, and the system stabilizes into a quasi-steady state. The temperature levels off at around 1450 K, while the pressure stabilizes near 24 GPa.

The high-temperature and high-pressure conditions observed in this stage promote severe plastic deformation, localized atomic rearrangement, and defect formation at the interface, which are critical for achieving strong metallurgical bonding in explosive welding. The plateau in both curves after ~20 ps indicates the end of the transient shock

regime and the transition to a post-impact state, which precedes unloading in subsequent stage.

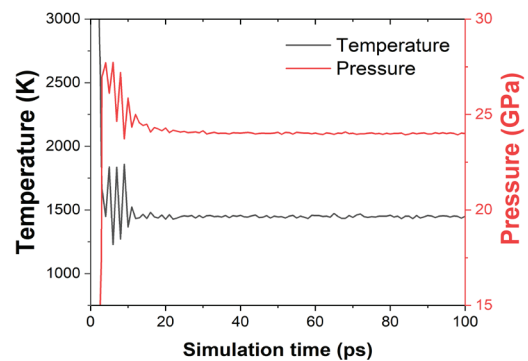


Figure 2. Temperature and pressure curves of simulation system during the loading stage.

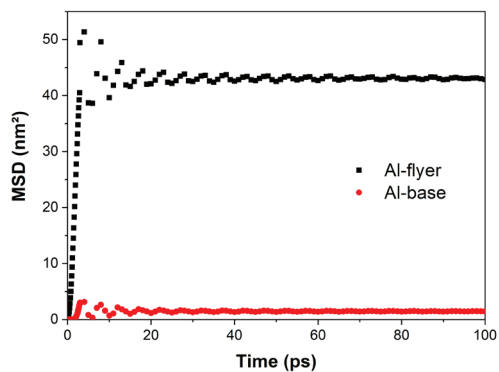
Figure 3 illustrates the evolution of mean square displacement (MSD) for Al-flyer and Al-base along the z-direction during both loading (a) and unloading (b) phases. MSD is a crucial indicator for tracking atomic mobility and diffusion behavior under dynamic loading conditions [8]. During the loading phase (Figure 3a), both Al-flyer and Al-base exhibit an initial rapid increase in MSD due to the sudden acceleration and impact-induced displacement of atoms. The Al-flyer shows a sharp rise to approximately 43 nm² within the first ~2 ps, after which its MSD curve stabilizes and remains nearly constant.

In contrast, the Al-base shows only minor oscillations around 2 nm² without any significant increase over time. This stabilization indicates that, although the system temperature exceeds the bulk melting point of aluminum (933.47 K), no noticeable diffusion occurs during the loading phase. The primary reason is that the extremely high pressure (~24 GPa) generated upon impact substantially elevates the melting point of aluminum, thus keeping the material in a solid or highly compressed solid-like state despite its elevated temperature.

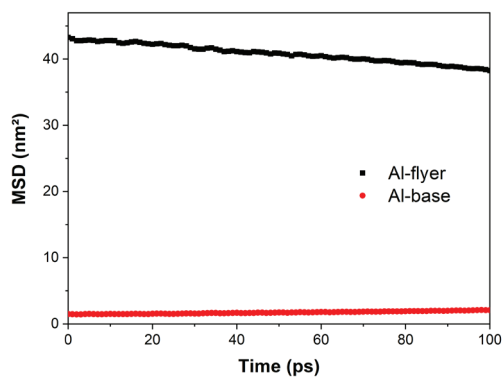
Table 1. MD Simulation Stages and Parameters

Stage	Ensemble	T / P	Time step (fs)	Damping parameters	Simulation time (ps)
Equilibration	NPT	300 K, 0 bar	1.0	$T_{damp}=1.0$ ps, $P_{damp}=0.05$ ps	10
Loading	NVE	-	1.0	-	Variable
Unloading	NVE	-	1.0	-	100
Cooling	NPT	300 K, 0 bar	1.0	$T_{damp}=1.0$ ps, $P_{damp}=1.0$ ps	100
Relaxation	NPT	300 K, 0 bar	1.0	$T_{damp}=1.0$ ps, $P_{damp}=1.0$ ps	100

Furthermore, the extremely short timescale of the loading stage (~ 10 ps) does not provide sufficient time for thermal diffusion to manifest significantly. This can be attributed to the combined effects of the extremely high impact pressure and the ultrashort loading timescale, which suppress melting even at temperatures above the ambient-pressure melting point. This behavior aligns with previous MD studies showing suppressed diffusion under shock compression conditions [9].



(a)



(b)

Figure 3. MSD curves for the loading (a) and unloading (b) phases in the z-direction.

In the unloading phase (Figure 3b), a different trend is observed. The MSD of the Al-flyer slightly decreases from its peak value (~ 43 nm²) to approximately 38.4 nm² over the unloading duration. This decrease is attributed to structural relaxation and elastic recovery after the removal of compressive stress. Simultaneously, the MSD of the Al-base shows a gradual linear increase with time, reaching about 2.1 nm² at the end of the unloading simulation (~ 100 ps). This slight increase suggests the onset of atomic diffusion and local

rearrangement as the high-pressure constraint is released, reducing the melting point back towards its ambient value. The thermal energy retained in the system (~ 1450 K) exceeds the melting point at atmospheric pressure, thus enabling localized melting and atomic mobility near the interface.

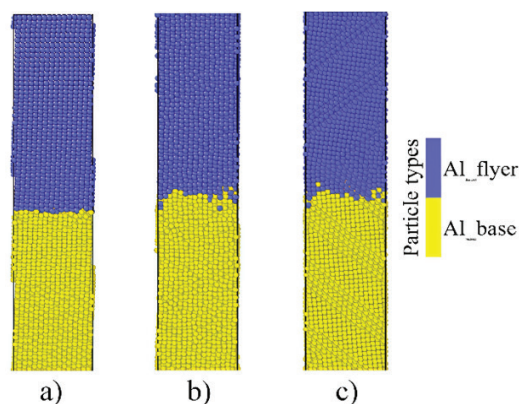


Figure 4. Atomic configurations at different stages of the explosive welding process: (a) immediately after collision, (b) after loading stage, and (c) after unloading stage.

Figure 4 illustrates the evolution of atomic configurations at three critical stages during the explosive welding process, with Al_flyer atoms colored in blue and Al_base atoms in yellow for clear visualization of interface morphology. In Figure 4a (immediately after collision), the interface between the flyer and base blocks remains relatively flat and well-defined. The Al_flyer and Al_base regions are distinctly separated, indicating that the impact has occurred but there is minimal intermixing or interfacial deformation at this very early stage. This is consistent with the extremely short timescale of initial collision where kinetic energy is largely concentrated in compressive deformation rather than diffusion.

In Figure 4b (after loading stage), noticeable morphological changes occur at the interface. The boundary between Al_flyer and Al_base becomes irregular, with the formation of small protrusions and indentations, suggesting localized plastic deformation and the onset of mechanical interlocking. Despite these structural changes, significant atomic interdiffusion is still absent, which corroborates the MSD results shown in Figure 3. The suppression of diffusion at this stage

is attributed to the high-pressure environment (~ 24 GPa) that effectively elevates the melting point of aluminum, thus maintaining solid-state bonding even though the system temperature is well above the standard melting temperature.

Finally, Figure 4c (after unloading stage) shows a more pronounced interfacial deformation compared to the loading stage. The interface exhibits deeper penetration of Al_flyer atoms into the Al_base region and vice versa, indicating the initiation of atomic mixing upon pressure release. This behavior is explained by the rapid reduction in melting point during unloading while the system retains high thermal energy (~ 1450 K), allowing localized melting and diffusion at the interface. The atomic distribution after unloading confirms that metallurgical bonding in explosive welding is facilitated not solely by impact-induced plastic deformation but also by thermally activated interdiffusion during the unloading and relaxation stages.

To quantify the atomic diffusion behavior near the weld interface, the Histogram modification function in OVITO was employed to extract the atomic concentration profiles along the Z-axis from the MD simulation results. Figure 5 presents the final distribution of Al-base and Al-flyer atom concentrations along the Z-direction. In this analysis, the diffusion layer thickness was defined as the region where the concentrations of both Al-base and Al-flyer atoms exceed 5%, indicating significant interfacial mixing between the two materials. The 5% concentration threshold was selected to exclude statistical noise in the concentration profiles and to identify only the region of effective atomic intermixing, which is consistent with previous molecular dynamics studies on explosive welding interfaces. As shown in Figure 5, the calculated thickness of the diffusion layer is approximately 12 Å. This result is consistent with previous MD simulation studies on explosive welding, which also reported diffusion layers with thicknesses on the order of a few angstroms to approximately 1 nm, corresponding to several atomic layers at the interface [1]. Such a thin diffusion region indicates that atomic mixing is highly localized, primarily driven by impact-induced plastic deformation rather than long-range thermal diffusion.

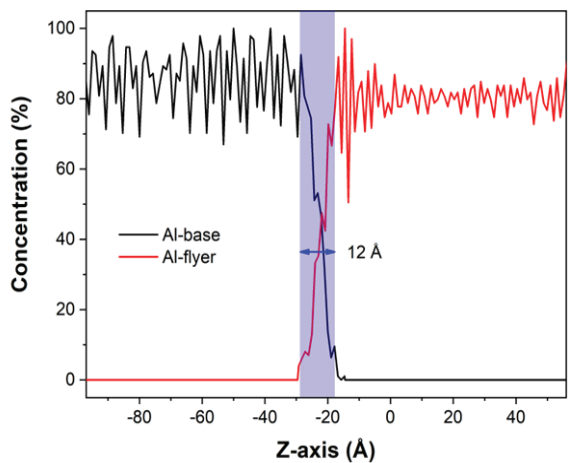


Figure 5. Main element distribution of MD simulation along the Z-axis.

In order to explore the effect of melting on atomic diffusion behavior during the explosive welding process, the radial distribution function (RDF) is used to analyze the atomic structures of each stage [10]. Figure 6 shows the RDF results for Al-flyer and Al-base atoms at different stages of the explosive welding process. At the initial stage, both regions exhibit identical RDF curves with sharp, periodic peaks characteristic of crystalline aluminum (FCC structure), with the first peak at ~ 2.85 Å. During the collision stage, RDF peaks decrease in intensity and broaden, indicating partial structural disturbance due to high-velocity impact. The Al-flyer shows a greater decrease and broader peaks compared to Al-base, suggesting more severe structural disruption in the flyer region. A slight leftward shift of the first peak also indicates local compression under shock loading.

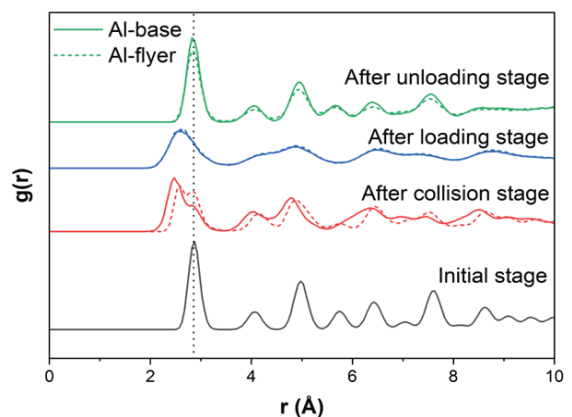


Figure 6. The RDF results of Al-flyer and Al-base at different stages.

In the loading stage, peak intensities further decrease and remain broad, implying persistent compressive stress and structural distortion. The Al-flyer maintains lower and broader peaks than Al-base, reflecting higher local deformation due to its initial kinetic energy upon impact. However, the presence of secondary peaks in both regions suggests that melting does not occur.

At the unloading stage, RDF peaks recover in intensity and sharpness, approaching their initial state, indicating partial recrystallization and structural relaxation upon pressure release. Nonetheless, Al-base peaks are sharper and more intense than those of Al-flyer, showing that Al-base regains a higher degree of crystalline order, while Al-flyer retains more residual defects and disorder. These results confirm that no significant melting occurs during explosive welding. Bonding arises mainly from plastic deformation and atomic rearrangement, consistent with the thin diffusion layer discussed in Figure 5. Moreover, the Al-flyer experiences greater structural distortion and retains more defects than Al-base due to its direct impact role in the welding process.

4. Conclusion

In summary, molecular dynamics simulations reveal that Al–Al explosive welding produces an

ultrahigh temperature above 2500 K and a peak pressure of about 27 GPa under a flyer velocity of ~ 29.7 Å/ps, resulting in severe plastic deformation while suppressing bulk melting due to the combined effects of high pressure and ultrashort impact duration. Atomic diffusion is strongly suppressed during loading, but becomes activated during unloading as pressure decreases and the system remains at an elevated temperature (~ 1450 K). RDF and MSD analyses confirm that bonding is governed mainly by solid-state plastic deformation with limited interdiffusion, forming a highly localized diffusion layer of approximately 12 Å. These findings provide quantitative guidance for selecting impact velocity and post-impact conditions in practical Al–Al explosive welding processes, in order to control interfacial plastic deformation and localized diffusion, thereby improving the reliability and quality of similar-metal cladding joints.

Conflict of Interest

The authors declare no conflict of interest.

Acknowledgment

This research is funded by Hung Yen University of Technology and Education under grant number UTEHY.L.2025.63.

Reference

- [1] Y. Ma, S. Zhang, T. Wang, Y. He, W. Chen, L. Liu, F. Liu, "Atomic diffusion behavior near the bond interface during the explosive welding process based on molecular dynamics simulations," *Materials Today Communications*, 31, p. 103552, 2022.
- [2] B. B. Sherpa, and S. Saravanan, "Review of the weldability window in explosive welding processes," *Journal of Alloys and Metallurgical Systems*, 9, p. 100150, 2025.
- [3] S. Bhat, Y. Khedkar, P. Prasad, "Advances in Explosive Welding of Dissimilar Metals: A Mini Literature Survey," *International Journal of Engineering Trends and Technology*, 72 (2), 108, 2024.
- [4] P. Kumar, M. Singh, S. Saravanan, S. Kumari, S. Kumar Ghosh, J. Deb Barma, R. K. Bhogendro Meitei, A. Biswas, "Study of explosive welding of Al 5052 and Al 1100 with stainless steel wire mesh interlayer," *Materials Today: Proceedings*, 2023,
- [5] V. I. Kuz'min, V. I. Lysak, S. V. Kuz'min, E. V. Kuz'min, "Formation characteristics and properties of an explosion-welded steel–aluminum composite with a diffusion barrier," *Composite Interfaces*, 31 (2), 215, 2024.
- [6] S. Mostafavi, F. Bamer, B. Markert, "Molecular dynamics simulation of interface atomic diffusion in ultrasonic metal welding," *The International Journal of Advanced Manufacturing Technology*, 118 (7), 2339, 2022.
- [7] R. R. Zope, and Y. Mishin, "Interatomic potentials for atomistic simulations of the Ti-Al system," *Phys. Rev. B*, 68 (2), 024102, 2003.

- [8] J. Zhou, N. Luo, H. Liang, W. Sun, “Multi-scale simulation and microstructure characteristics of TC4 ELI/Al 6013 plates by explosive welding,” *Journal of Manufacturing Processes*, 124, 1180, 2024.
- [9] C. Pu, X. Yang, D. Xiao, J. Cheng, “Molecular dynamics simulations of shock melting in single crystal Al and Cu along the principle Hugoniot,” *Materials Today Communications*, 26, 101990, 2021.
- [10] C. Shi, X. Luo, Z. Sun, H. Wang, H. Shi, J. Jiang, “Experimental and numerical study of interface and mechanical properties of TA1/5083/TA1 vacuum creep pressure bonding composites,” *Journal of Manufacturing Processes*, 124, 458, 2024.

NGHIÊN CỨU Ở CẤP NGUYÊN TỬ QUÁ TRÌNH HÀN NỔ Al/Al BẰNG MÔ PHỎNG ĐỘNG LỰC HỌC PHÂN TỬ VỀ CƠ CHẾ LIÊN KẾT VÀ KHUẾCH TÁN TẠI GIAO DIỆN

Tóm tắt:

Hàn nổ (EXW) được sử dụng rộng rãi để ghép nối các kim loại giống và khác nhau, tuy nhiên cơ chế ở cấp độ nguyên tử của nó vẫn chưa được nghiên cứu rõ. Trong nghiên cứu này, mô phỏng động lực học phân tử đã được thực hiện để khảo sát quá trình hàn nổ nhôm–nhôm bằng cách sử dụng thế EAM (Embedded Atom Method). Kết quả cho thấy tác động của flyer làm nhiệt độ vượt quá 2500 K và áp suất đạt đỉnh khoảng ~27 GPa, gây ra biến dạng dẻo nghiêm trọng mà không xảy ra nóng chảy khối. Phân tích dịch chuyển bình phương trung bình (MSD) và nồng độ nguyên tử cho thấy có khuếch tán trong giai đoạn tải, trong khi giai đoạn dỡ tải thúc đẩy sự trộn lẫn tại giao diện, tạo ra một lớp khuếch tán mỏng khoảng ~12 Å. Phân tích hàm phân bố xuyên tâm (RDF) xác nhận rằng liên kết được hình thành chủ yếu bởi biến dạng dẻo ở trạng thái rắn và sự sắp xếp lại cục bộ của nguyên tử. Những phát hiện này cung cấp hiểu biết ở cấp nguyên tử về quá trình hàn nổ nhôm–nhôm, hỗ trợ tối ưu hóa quy trình để tạo các mối nối kim loại giống nhau có độ bền tin cậy.

Từ khóa: Hàn nổ; Mô phỏng động lực học phân tử; Liên kết nhôm–nhôm; Khuếch tán tại giao diện.